

*Advances in High Pressure Science & Technology*

*Edited by A.K.Singh*

Tata McGraw-Hill, New Delhi

## **Microstructural Studies on the Pressure-Temperature Treated Nickel Specimens**

*T.A.Bhaskaran, M.A.Parameswara and Murali Mohan*

Materials Science Division, National Aerospace Laboratories, Bangalore 560 017

### **Abstract**

Annealed nickel wire-specimens have been subjected to  $\sim 5.5$  GPa and to different temperatures in the range 550-750 K using an externally heated tungsten carbide opposed anvil apparatus with talc as a pressure transmitter. The microhardness measurements on the recovered specimens exhibited an increase in the range 15-35 % in the values over those obtained on the as-annealed specimens. This suggests work-hardening effects during the pressurization. However, the optical micrographs of these specimens do not show any evidence of plastic deformation. The transmission electron microscopic studies on annealed nickel wafers recovered after pressurization (2-10 GPa at 300 K) under talc pressure medium provide microstructural evidences for the deformation of the specimen. The deformation microstructure consists of a sequential evolution, with increasing pressure, of (i) dislocation cells, (ii) dense dislocation walls, and (iii) features leading to the formation of subgrains. This suggests that the plastic deformation of the specimens increases with increase in pressure. The dislocation density in the annealed specimens before pressurization is  $\sim 2 \times 10^8 \text{ cm}^{-2}$ , and increases to  $\sim 10^{11} \text{ cm}^{-2}$  after pressurization.

### **1 Introduction**

Tungsten carbide opposed anvil setup of the Bridgman type has been widely used to study the pressure-temperature ( $p$ - $T$ ) behaviour of the electrical resistivity of metallic specimens. In this device, the pressure is transmitted on to the specimen, contained in a compressible gasket, by a pressure transmitter. When a solid is used as a pressure transmitting medium, the applied load generates a quasi-hydrostatic pressure on the specimen. The stress field around the specimen deviates<sup>1</sup> from the hydrostatic pressure in two ways. Firstly, the use of a solid pressure medium leads to a

pressure gradient in the radial direction. The magnitude and direction of the pressure gradient depend on the shear strength of the pressure transmitting medium and the dimensions of the gasket. Secondly, in the presence of a solid pressure transmitting medium, the axial stress component ( $\sigma_a$ ) exceeds the radial stress component ( $\sigma_r$ ); the difference ( $\sigma_a - \sigma_r$ ) is termed the uniaxial stress component<sup>2-5</sup> (USC) and is of the order of the yield strength of the pressure transmitting material. The stress distribution on the specimen may be regarded as a superimposition of a USC on the predominantly hydrostatic component of pressure. Hence a specimen in such a stress field is likely to undergo a mechanical deformation which is absent under truly hydrostatic pressure conditions.

The  $p$ - $T$  dependence of the electrical resistance of polycrystalline nickel wire specimens, across the magnetic transition, obtained using the opposed anvil apparatus with pyrophyllite gasket and talc as the pressure transmitter has been discussed in an earlier study<sup>6</sup> where the  $p$ - $T$  behaviour of Ni was found to exhibit all the features similar to that obtained under a truly hydrostatic medium<sup>7</sup>. However, the magnitudes of the pressure coefficient of resistance,  $|\beta| = |[-dR/dp]/R_o|$ , of the as-received (A) and the annealed specimens (B) were different especially at temperatures greater than the Curie temperature.  $\beta$  of specimen A was always closer to the hydrostatic value, but that of specimen B was consistently lower by a factor  $\sim 1.5$ . It was expected that the large plastic deformation of specimen B relative to specimen A, during pressurization, would increase  $R$ , and thereby lower  $\beta$ .

Subsequently, the microhardness ( $H_K$ ), and the optical microscopic (OM) investigations of the specimens<sup>6</sup> recovered after the  $p$ - $T$  treatment has been carried out, and the results are discussed in this paper. While the  $H_K$  values suggest a relatively large plastic deformation of specimen B on pressurization, no evidence of such effects is revealed in the optical micrographs. This necessitated a systematic microstructural analysis of the pressurized specimens by transmission electron microscopy (TEM). As a part of this study, firstly we have carried out a TEM study on specimens B recovered after pressurization to desired values in the range 2-10 GPa at 300 K. The evolution of the deformation microstructure and the changes in the dislocation densities are also discussed in this paper.

## 2 Experimental details

### 2.1 Starting material

The Ni-wire (0.1 mm in diameter), 99.999 % pure from Johnson Matthey Chemicals, was used as the starting material in the present experiments. The OM studies were carried out on wire specimens. For TEM studies, the wire was flattened to  $\sim 0.07$  mm thickness and  $\sim 5$  mm in breadth, and from these, circular discs  $\sim 3$  mm in diameter were punched out. The specimens were annealed in quartz tubes, sealed under a vacuum of  $10^{-5}$  Torr, at 1000 K for 4 h using Ti as a getter material. The as-received and the annealed specimens are referred to as specimen A and specimen B respectively.

### 2.2 High pressure - high temperature experiments

A tungsten carbide opposed anvil device (anvil face of 12.7 mm diameter) capable of generating pressures up to 10 GPa with pyrophyllite gasket and talc as the pressure transmitter was used to pressurize the specimens. The details of the high pressure - high temperature cell, the pressure calibration, and the temperature measurements are described elsewhere<sup>1,6,8</sup>. The wire specimens for OM studies were those which were recovered after the isothermal measurements<sup>6</sup> of electrical resistance up to 5.5 GPa and 750 K. The pressurized region of the wire was  $\sim 20$  mm long and bent in a zigzag ( $2.5 \times 3$  mm<sup>2</sup>) form. The disc specimens for TEM studies were also pressurized in a similar way at 300 K to desired values (2-10 GPa), held at that pressure for  $\sim 30$  minutes, and then unloaded. The specimens were recovered after the pressure dropped to the atmospheric value. The uncertainty in the specimen pressure was  $\pm 0.1$  GPa at 10 GPa. In the high temperature experiments, the specimen temperature was controlled to  $\pm 1$  K at the desired value.

### 2.3 Specimen preparation for microscopic studies

The  $p$ - $T$ -treated Ni wire specimens were electrolytically plated with Cu to a thickness of  $\sim 250$   $\mu\text{m}$ . The plated specimens were allowed to set in a polymer resin base. After setting, the epoxy was ground till a longitudinal section of the Ni wire was well exposed. This surface was polished using diamond paste ( $\sim 1$   $\mu\text{m}$ ) and alumina powder ( $\sim 0.05$   $\mu\text{m}$ ), carefully etched for  $\sim 30$  s in a mixture of nitric acid and acetic acid (1:1 by volume), and observed in a Neophot-2 microscope.

The TEM specimens were prepared by electropolishing the pressure-treated disc

specimens in a twin-jet Tenupol unit. The composition of the electrolyte was a mixture of 26 % nitric acid and 74 % methanol. The electrolyte was maintained at  $243 \pm 2$  K, and a d.c. potential of  $\sim 35$  V was applied. The specimens after perforation were thoroughly cleaned in alcohol and stored in air tight vials. These (wafers of thickness 1000-1500 Å) were examined under a JEOL-2000 FX TEM (operating voltage 200 kV), and standard bright field images were recorded under optimum diffraction conditions.

## 2.4 Hardness measurements

The Knoop hardness measurements were made on polished wire specimens using the Epival (mhp-160) microhardness tester with a test load of 40 gf. Since, typically, different regions of the pressurized wire were simultaneously exposed, the indentations were made at several random locations. A typical indentation on the specimen is shown in Fig 1'. The length,  $l$ , of the long diagonal was measured in each case. The Knoop hardness,  $H_K$ , was calculated using the standard expression

$$H_K = \frac{14228.8 \times L}{l^2} \quad (1)$$

where  $H_K$  is in  $\text{kg}/\text{mm}^2$ ,  $L = 40$  gf and  $l$  in  $\mu\text{m}$ .

## 3 Results and discussion

### 3.1 Optical metallographic studies

The microstructure of the specimen A (Fig 2) shows the flow lines characteristic of the extruded specimen; the grains are elongated in the direction of extrusion. Fig 3 shows the microstructure of the specimen B exhibiting recrystallized equiaxed grains. The present annealing conditions are sufficient to cause the disappearance of the texture (Fig 2), and lead to the growth of recrystallized grains (Fig 3). The microstructure of a typical specimen B, recovered after subjecting it to 5.5 GPa and 570 K (Fig 4), is similar to that observed for specimen B in the un-pressurized condition (Fig 3). The optical micrographs do not reveal any evidence of the plastic deformation of the specimens.

The range of  $H_K$  values of the specimen B recovered after pressurization to 5.5 GPa under isothermal conditions at different  $T$  is shown in Table 1. Also shown are

Fig.1

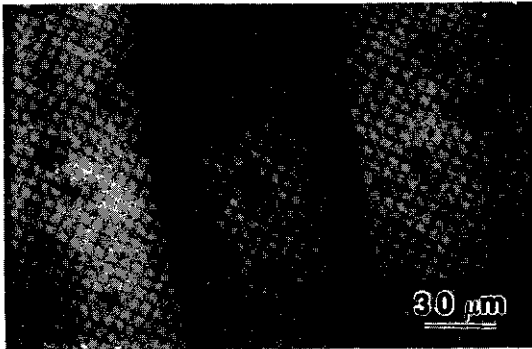


Fig.2



Fig.3

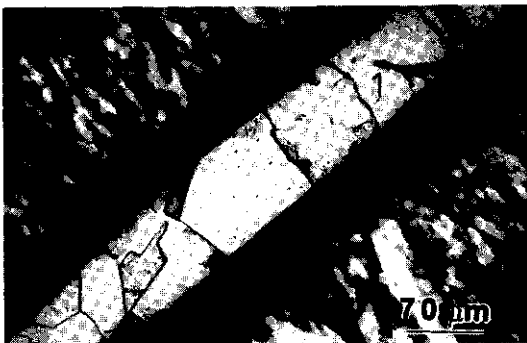


Fig.4

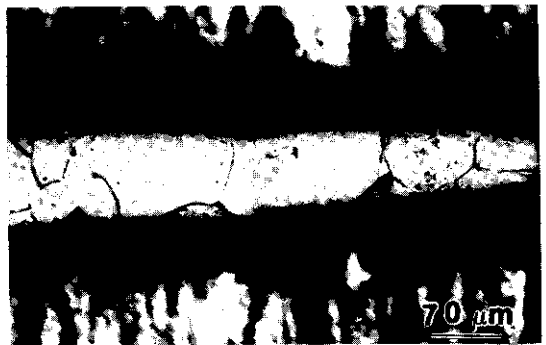


Figure 1: *Typical Knoop indentation on a polished Ni specimen.*

Figure 2: *Flow lines in the as-received Ni wire.*

Figure 3: *Recrystallized equiaxed grains in a typical annealed specimen.*

Figure 4: *Microstructure of the specimen recovered after pressurization to 5.5 GPa and 570 K.*

the values before the  $p$ - $T$  treatment. The present  $H_K$  values at ambient conditions are in good agreement with the range of values 60-80 kg mm<sup>-2</sup> reported earlier<sup>9</sup> for polycrystalline annealed Ni specimens of 99.9 % purity. It is seen that the  $H_K$  increases by  $\sim 15$  % for the specimens pressurized at  $\sim 570$  K as compared to  $\sim 34$  % for those pressurized at  $\sim 730$  K. The increase in  $H_K$  suggests that the specimens undergo plastic deformation on pressurization, and the extent of plastic deformation is larger at higher temperatures. Further, considering that the Curie temperature ( $T_c$ ) of Ni at atmospheric pressure is  $\sim 630$  K and the value<sup>10</sup> of  $dT_c/dp = 3.3$  K GPa<sup>-1</sup>, it is interesting to note that the increase in  $H_K$  arising from pressurization is larger in the paramagnetic phase of Ni than in the ferromagnetic phase.

Table 1: Knoop hardness,  $H_K$ , values of the annealed Ni specimens recovered after  $p$ - $T$  treatment.

$p$ - $T$ conditions	$H_K$ (kg/ mm <sup>2</sup> )	% increase in hardness
ambient	74-81	0
5.5 GPa-570 K	87-91	$\sim 15$
5.5 GPa-697 K	98-103	$\sim 30$
5.5 GPa-730 K	101-106	$\sim 34$

### 3.2 TEM studies

The transmission electron micrograph (Fig 5) of the specimen B shows a longitudinal section of a grain with straight boundaries; the lateral dimension of the grain is  $\sim 15$   $\mu$ m. The microstructure does not show dislocation cells or well defined dislocation segments. However, some remnant dislocations after annihilation are visible.

The bright field images of the specimen B recovered after pressurization to 2 GPa at 300 K are shown in Figs 6(a) and (b). Dislocation tangles and dislocation forests are clearly seen in Fig 6(a), this region also exhibits a high density of dislocations

(Table 2). The deformation microstructure in Fig 6(b) consists of dislocation cells, and dark bands of high density of dislocations. The dislocation cells are equiaxed and formed in different volume elements inside the grain. The long dark bands subdividing the dislocation cells are the dislocation dense walls (DDW). It is noticed that the DDW sweeps several dislocation cells which share the DDW as a common boundary. That the dark bands are indeed the DDWs and not the grain boundaries is corroborated by the fact that the spacing between them is  $\sim 5 \mu\text{m}$ , whereas the grain size is much larger.

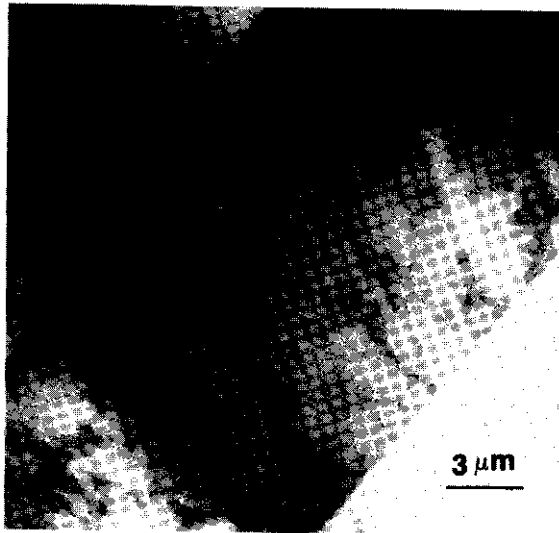


Figure 5: *Transmission electron micrograph of the annealed Ni specimen; dislocation cells are absent.*

Figs 7(a) and (b) are the micrographs of the specimen B recovered after pressurization to 4 GPa. Well developed equiaxed dislocation cells are seen in Fig 7(a). The DDWs are also seen in Fig 7(b). Further, Fig 7(b) shows the presence of thicker DDWs. This feature points to a higher level of deformation in the specimens recovered after pressurization to 4 GPa than in those pressurized to 2 GPa.

The deformation microstructure of the specimen recovered after pressurization to 10 GPa is shown in Fig 8. A noticeable difference between this and the microstruc-

tures at 2 and 4 GPa is that the dislocation cells are clearly absent even though the density of dislocations is higher (Table 2). This is believed to be due to the earlier stages of subgrain formation which is a still higher level of deformation than those observed in the specimens recovered after pressurization at 4 GPa.

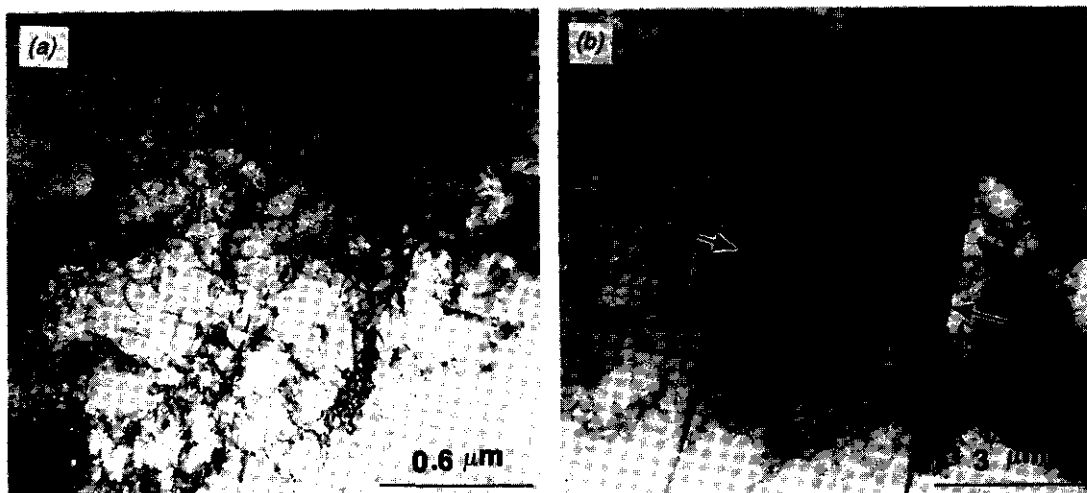


Figure 6: (a) Dislocation tangles and forests (b) Dislocation cells and dense dislocation walls (indicated by arrows) in a specimen recovered after pressurization to 2 GPa at 300 K.

It is pertinent to discuss here the general features of the deformation microstructures<sup>11–13</sup> that evolve during the different stages of plastic deformation of metals and alloys. During the deformation of a polycrystalline material, the grains are first subdivided into rotated volume elements. The different features such as the dislocation cells, DDWs, microbands and subgrains evolve progressively with the increase in the levels of deformation. The dislocation cells, rotated with respect to one another, are a type of dislocation arrangement in which the density of dislocations is very high at the cell boundaries as compared to the cell interior. The DDWs and the microbands are planar defects separating two regions of a lattice misoriented with respect to each other in which different slip systems operate. These regions also help to accommodate the inhomogeneous strains occurring during deformation in different



regions of a grain. The misorientation between the cell walls is smaller compared to that between the DDWs. The subgrains result when the misorientations across the dislocation boundaries become larger. In the light of these discussions, a comparison of the microstructures (Figs 6-8) points to the expected trend that the deformation of the specimen increases with increase in pressure. Further, the evolution of the DDWs in the microstructures of the deformed specimens indicates the presence of inhomogeneous strains during pressurization under a solid pressure medium.

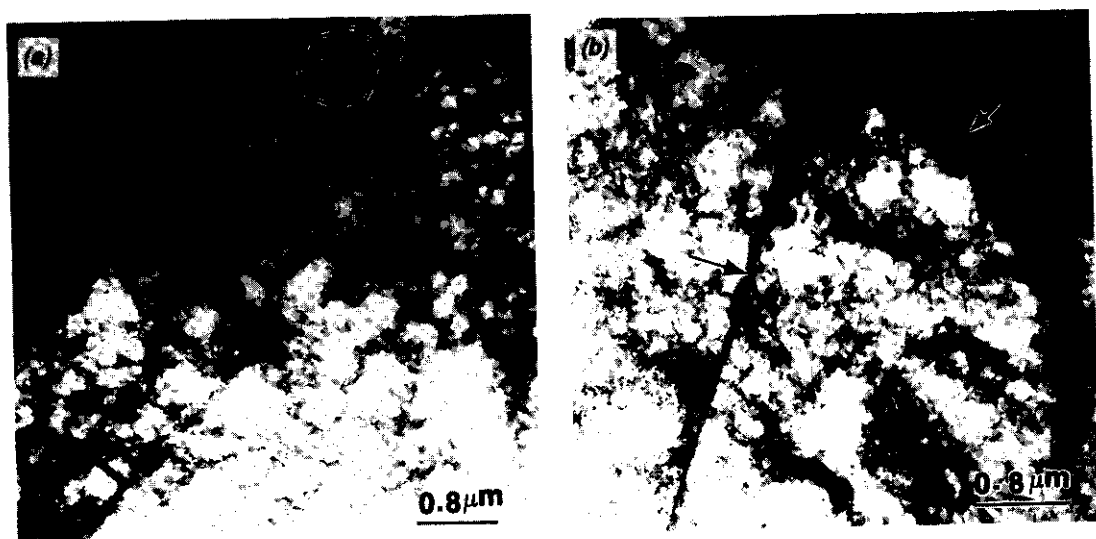


Figure 7: (a) Well defined equiaxed dislocation cells (boundary of a typical cell is marked) (b) dense dislocation walls (thick DDWs are marked by the arrow on the right), in a specimen recovered after pressurization to 4 GPa at 300 K.

The deformation microstructures obtained in the present study are similar to those obtained in earlier studies<sup>14,15</sup> where the specimens were grossly deformed by different techniques. Hughes and Hansen<sup>14</sup> reported the formation of dislocation cells, DDWs and microbands in Ni specimens subjected to rolling and torsion at atmospheric pressure. The specimens in these experiments were deformed to a strain corresponding to von Mises strain of 0.3. It must be noted that in the present experiments, the Ni specimens were embedded in talc discs during pressurization and the shear stresses

are limited by the shear strength of talc. Further the magnitude of the USC, determined as twice the shear strength of talc, is  $\sim 0.05$  GPa at 5 GPa. Hence the plastic strains in the specimens are expected to be much smaller than 0.3. It is therefore likely that strains required to cause a given extent of deformation in the specimen are smaller when the specimen is under pressure than when it is at atmospheric pressure. Jesser and Kuhlmann-Wilsdorf<sup>15</sup> severely deformed Ni specimens in shear under high normal pressures (up to 12 GPa) between a pair of tungsten carbide anvils. The microstructure of the deformed specimens revealed a high density of dislocations; however, no well defined dislocation cells were observed. It is possible that in these specimens, the deformation of the specimen is so large that it might have reached the stage of subgrain formation.

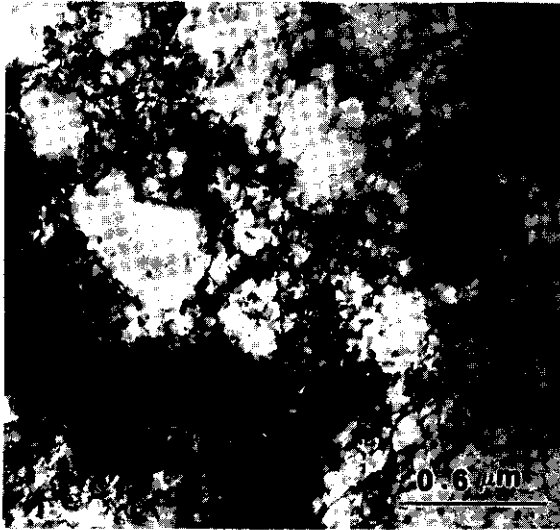


Figure 8: *Deformation microstructure of a specimen recovered after pressurization to 10 GPa; dislocation cells are absent.*

### 3.3 Dislocation densities

The dislocation densities were measured from the TEM micrographs by the intercept method. For this, the wafer specimen was tilted in the microscope so that a majority of dislocations exhibited maximum contrast, and thereby became visible.

The number,  $N$ , of dislocations intersecting an arbitrary straight line of length,  $x$ , (superimposed on the micrograph) was measured over different regions of the micrographs. The density,  $\rho$ , of dislocations was calculated using the expression  $\rho = 2N/xt$ , where  $t$  is the thickness of the foil;  $t$  is assumed to be  $1000 \text{ \AA}$ . The values of  $\rho$  for different specimens are shown in Table 2. Also shown are the values of  $\rho$  for the annealed specimen before pressurization. The value of  $\rho = 10^8 \text{ cm}^{-2}$  is typical of such values reported earlier<sup>16</sup> for annealed specimens. Further,  $\rho$  increases by a factor  $\sim 10^2$  on pressurization, and this is attributed to work hardening effects arising from the plastic deformation of the specimen. The values of  $\rho = 10^{10} - 10^{11} \text{ cm}^{-2}$  obtained in the present studies for the pressurized specimens are of the same order of magnitude as those obtained earlier<sup>15</sup> for the grossly deformed Ni specimens.

Table 2: Mean dislocation densities of the annealed Ni specimens recovered after pressurization at 300 K.

Pressure	$\rho \text{ (cm}^{-2}\text{)}$
ambient	$2.2 \times 10^8$
2 GPa	$2.5 \times 10^{10}$
4 GPa	$3.7 \times 10^{10}$
10 GPa	$8.0 \times 10^{10}$

### 3.4 Some comments

The deformation microstructure, and the increase in  $\rho$  obtained through TEM studies clearly provide evidences for the plastic deformation of annealed specimens(B) during pressurization under a solid pressure medium at 300 K. For the  $p$ - $T$  treated specimens, no visible changes in the microstructure, as compared to those of the starting specimens, were observed in the optical micrographs. The evidence of plastic deformation, due to pressurization, in these specimens is only through the increase in  $H_K$  over the values obtained in the unpressurized condition. In this context, the TEM studies on the  $p$ - $T$  treated specimens will be of interest. However, it is tempting

to attribute the observed increase in  $H_K$  values in the  $p$ - $T$  treated specimens to a possible increase in  $\rho$  during pressurization at higher  $T$ .

The values of  $\beta$ , at 300 K, of specimens A and B obtained earlier<sup>6</sup> were similar, the average value being  $-0.019 \pm 0.001 \text{ GPa}^{-1}$ . Further, this value is in close agreement with the value of  $-0.0182 \text{ GPa}^{-1}$  obtained at 300 K under a truly hydrostatic medium<sup>7</sup>. This points to the fact that the plastic deformation of specimen B during pressurization, as evidenced by the present study, does not seem to affect the resistance-pressure behaviour at 300 K.

## Acknowledgements

We thank Dr A.K.Singh for his encouragement and support. Thanks are also due to Prof S.Ranganathan, Department of Metallurgy, IISc, Bangalore for providing the JEOL-2000 FX TEM facility. We thank Dr.R.V.Krishnan for a critical reading of the manuscript.

## References

1. A.K.Singh, *Mat.Sci.Forum*, (Transtech-Switzerland), **3**, 291 (1985).
2. A.K.Singh and G.C.Kennedy, *J.Appl.Phys.*, **45**, 4686 (1974).
3. S.Usha Devi and A.K.Singh, *Physica*, **139 & 140B**, 922 (1986).
4. A.K.Singh, *J.Appl.Phys.*, **73**, 4278 (1993).
5. A.K.Singh and C.Balasingh, *J.Appl.Phys.*, **75**, 4956 (1994).
6. Murali Mohan, M.A.Parameswara and A.K.Singh, in *Recent Trends in High Pressure Research*, Ed. A.K.Singh (Oxford & IBH, New Delhi) 461 (1992).
7. B.Sundquist, *Phys.Rev.(B)*, **38**, 12283 (1988).
8. A.K.Singh, Murali Mohan and C.Divakar, *J.Appl.Phys.*, **54**, 5721 (1983).
9. A.A.Invan'ko, in *Handbook of hardness data*, Ed. G.V.Samsonov, Translated from Russian, Isreal Programme for Scientific Translations, 17 (1971).
10. J.M.Leger, C.Susse and B.Vodar, in *Accurate Characterization of the high pressure environment*, Ed. E.C.Lloyd, (NBS-Special Publication 326), 251 (1968).
11. D.A.Hughes, *Scripta Met.et.Mater.*, **27**, 969 (1992).
12. N.Hansen, *ibid*, 947.
13. Doris Kuhlmann-Wilsdorf, *ibid*, 951.
14. D.A.Hughes and N.Hansen, *Mat.Sci.Tech.*, **7**, 544 (1991).
15. W.A.Jesser and D.Kuhlman-Wilsdorf, *Mat.Sci.Engg.*, **9**, 111 (1971).
16. R.W.Margevicius and J.J.Lewandowski, *Acta Metall.Mater.*, **41**, 485 (1993).